A&A 650, A160 (2021)
https://doi.org/10.1051/0004-6361/202039991

Astronomy & Astrophysics

Study of Fischer–Tropsch-type reactions on chondritic meteorites

V. Cabedo[1,3], J. Llorca[2], J. M. Trigo-Rodriguez[3,4], and A. Rimola[5]

[1] Astrophysics department, CEA/DRF/IRFU/DAp, Université Paris Saclay, UMR AIM, 91191 Gif-sur-Yvette, France
e-mail: victoria.cabedo@cea.fr
[2] Institut de Tècniques Energètiques and Departament d'Enginyeria Química, Universitat Politècnica de Catalunya, Barcelona, Catalonia, Spain
[3] Institute of Space Sciences (CSIC), Meteorites, Minor Bodies and Planetary Sciences Group, Campus UAB, Carrer de Can Magrans, s/n, 08193, Barcelona, Catalonia, Spain
[4] Institut d'Estudis Espacials de Catalunya (IEEC), Gran Capità, 2 - baix, 08034, Barcelona, Catalonia, Spain
[5] Departament de Química, Universitat Autònoma de Barcelona, 08193 Bellaterra, Catalonia, Spain

Received 25 November 2020 / Accepted 11 May 2021

ABSTRACT

Context. How simple organic matter appeared on Earth and the processes by which it transformed into more evolved organic compounds, which ultimately led to the emergence of life, is still an open topic. Different scenarios have been proposed, the main one assumes that simple organic compounds were synthesized, either in the gas phase or on the surfaces of dust grains, during the process of star formation and they were incorporated into larger bodies in the protoplanetary disk. The transformation of these simple organic compounds in more complex forms is still a matter of debate. Recent discoveries have pointed to catalytic properties of dust grains present in the early stellar envelope, which can nowadays be found in the form of chondrites. The significant infall of chondritic meteorites during the early periods of Earth suggests that the same reactions could have taken place in certain environments on the Earth's surface, with conditions more favorable for organic synthesis.
Aims. This work attempts to synthesize simple organic molecules, such as hydrocarbons and alcohols via Fischer–Tropsch-type reactions supported by different chondritic materials under early-Earth conditions, to investigate if organic synthesis can likely occur in this environment and to determine what the differences are in selectivity when using different types of chondrites.
Methods. Fischer–Tropsch-type reactions are investigated from mixtures of CO and H_2 at 1 atm of pressure on the surfaces of different chondritic samples. The different products obtained are analyzed in situ by gas chromatography.
Results. Different Fischer–Tropsch reaction products are obtained in quantitative amounts. The formation of alkanes and alkenes being the main processes. The formation of alcohols also takes place in a smaller amount. Other secondary products were obtained in a qualitative way.
Conclusions. Chondritic material surfaces have been proven as good supports for the occurrence of organic synthesis. Under certain circumstances during the formation of Earth, they could have produced a suitable environment for these reactions to occur.

Key words. astrochemistry – meteorites, meteors, meteoroids – planetary nebulae: general

1. Introduction

Life on Earth likely arose from a series of particular conditions, which have yet to be unambiguously determined. It has been envisioned that the early Earth was exposed to different sources of energy, such as light, heat, and reduction–oxidation (redox) potentials. Such an environment also received a large flux of extraterrestrial material, at least until the end of the late heavy bombardment (LHB, Bottke et al. 2012). At some point, the conditions in the atmosphere and surface of our planet might have promoted an increase in molecular complexity (Rotelli et al. 2016) which, later on, allowed the recombination of organic molecules to form more complex, interacting and self-replicating systems (Walde 2005; Shulze-Makuch & Irwin 2008).

The synthesis of interstellar complex organic molecules (iCOMs) in the solar nebula and during the process of star formation has been extensively studied during recent years (Herbst 2017). The simplest organic compounds, such as formaldehyde (H_2CO) and methanol (CH_3OH), and other iCOMS, including acetaldehyde (CH_3CHO) and formamide (NH_2CHO) for instance, have been repeatedly observed from starless cores to star forming regions (Vasyunina et al. 2014; López-Sepulcre et al. 2015; Bianchi et al. 2018; McGuire 2018; van Gelder et al. 2020). Robust pieces of evidence indicate that the formation of iCOMs takes place on the surface of interstellar grains (Kress & Tielens 2001; Sekine et al. 2006; Linnartz et al. 2015; Oberg 2016, Enrique-Romero et al. 2019; Zamirri et al. 2019; Martín-Doménech et al. 2020), which with time will coagulate and form the embryos of rocky planets and minor bodies.

Chondrites are a class of meteorites that come from undifferentiated bodies (they never melted), such as small asteroids or comets, and they have suffered very low chemical or thermal alteration processes (Zolensky et al. 2008). Chondrites come from the direct accretion of the primordial materials forming the protoplanetary disk, so they are believed to be the most pristine samples of the dust grains forming our early Solar System (Weisberg et al. 2006; Trigo-Rodriguez 2015) preserving their primordial components: metal grains, sulfides, and igneous silicate-rich spherules called chondrules (hence the name chondrites). Particularly interesting are carbonaceous chondrites

(CCs) since they contain about 1–4% of carbon in mass (Remusat et al. 2007; Alexander et al. 2017), which is found in the form of organic matter aggregates (Trigo-Rodriguez et al. 2019). This organic matter is thought to have been synthesized in the solar nebula, some of these reactions being catalyzed by the surfaces of the metallic phase present in the dust (Llorca & Casanova 2000).

Surface reactions in solid-dry environments can play a central role in the synthesis of biomolecular precursors and other large complex organic molecules of extrasolar origin, which have been identified in undifferentiated meteorites (Ehrenfreund & Charnley 2000; Sephton 2002; Botta & Bada 2002). Indeed, different studies demonstrate that important prebiotic molecules, including amino acids (Bernstein et al. 2002; Muñoz Caro et al. 2002; Elsila et al. 2007; Nuevo et al. 2008; Lee et al. 2009), can be formed by processing of interstellar ices (Ciesla & Sandford 2012; Fedoseev et al. 2015, 2017; Chuang et al. 2015, 2017). More recently, nonenergetic ice chemistry (i.e., without the need of energetic external triggers processing the ice) has been shown to be also operative in the formation of glycine (Krasnokutski et al. 2020; Ioppolo et al. 2021). However, investigations on the synthesis of prebiotic compounds on meteoritic minerals and/or analogs under dry conditions (i.e., through gas-surface reactions) is practically missing.

Since H_2 and CO are the most abundant gas-phase compounds in most of the astrophysical environments, along with the fact that metallic components usually used as catalytic supports are commonly found in meteoritic materials, gas-surface Fischer–Tropsch-type (FTT) reactions are invoked here as possible synthetic routes for part of the organic content (i.e., hydrocarbons and alcohols) identified in these asteroidal bodies (Ferrante et al. 2000; Sekine et al. 2006). The Fischer–Tropsch synthesis consists of a set of chemical reactions that produce hydrocarbons and fuels from mixtures of CO and H_2 (see Eqs. (1) and (2)). Additionally, it can also produce secondary reactions such as the formation of alcohols (Eq. (3)) or the disproportion of CO (Eq. (4), Schulz 1999; Mahmoudi et al. 2017). FTT processes proceed under the presence of a metal catalyst, generally Fe, Co, Ni and Ru. The mechanism of the reaction and the product selectivity and distribution vary depending on the metal used as support and on the reaction conditions (Mahmoudi et al. 2017) as follows:

$$n\mathrm{CO}_{(g)} + (2n+1)\mathrm{H}_{2(g)} \rightleftharpoons \mathrm{C}_n\mathrm{H}_{2n+2_{(g)}} + n\mathrm{H}_2\mathrm{O}_{(g)} \quad (1)$$

$$n\mathrm{CO}_{(g)} + (2n)\mathrm{H}_{2(g)} \rightleftharpoons \mathrm{C}_n\mathrm{H}_{2n_{(g)}} + n\mathrm{H}_2\mathrm{O}_{(g)} \quad (2)$$

$$n\mathrm{CO}_{(g)} + (2n)\mathrm{H}_{2(g)} \rightleftharpoons \mathrm{C}_{(n)}\mathrm{H}_{2n+1}\mathrm{OH}_{(g)} + (n-1)\mathrm{H}_2\mathrm{O}_{(g)} \quad (3)$$

$$2\mathrm{CO}_{(g)} \rightleftharpoons \mathrm{C}_{(s)} + \mathrm{CO}_{2(g)}. \quad (4)$$

The advent of organic chemical reactions in primordial grains of the solar nebula and the protoplanetary disk is of fundamental relevance as these materials were lately processed to form the seeds of planets, comets and meteorites (Brearley & Jones 1998). Moreover, the flux of chondritic material was important during the early periods of the Earth, which could provide the support and conditions necessary for these reactions to occur. The vapor clouds produced by the impacts of these bodies and the presence of these particular metal alloys, with the high pressure and high temperature conditions, could have established an adequate environment for complex chemistry to take place.

If FTT reactions can be extrapolated to environments similar to the available conditions present in the primeval Earth, chondritic meteorites could be responsible not only for bringing large amounts of organic material and water to the protoplanet, but also for promoting reactions of paramount astrobiological relevance in the emergence of prebiotic chemistry. Therefore, the aim of this work is to explore this possibility by simulating FTT processes in an environment similar to the primeval atmosphere of Earth.

2. Experimental procedure

2.1. Sample description and preparation

Two different meteoritic samples were used to prove their surface activity, provided by different collections and chosen by their availability. Samples of CCs and ordinary chondrites (OCs) have been chosen because of their primitive composition, with an isotopic composition similar to solar, and their relative low degree of alteration. These characteristics make them good exemplars of the dust present in the protoplanetary disk. Moreover, both classes cover an important percentage of the recovered meteorites that fall into Earth's surface, and therefore, by extrapolation, they are also good examples of the kind of materials that fell during the early stages of Earth's formation.

KG 007 is an OC of subtype H and petrological type 6 (Ruzicka et al. 2014). Those are distinguished by presenting subsolar Mg/Si and refractory/Si ratios, to exhibit oxygen isotope composition above the terrestrial fractionation line and to contain a large volume percentage of chondrules, with only 10–15 vol.% of a fine-grained matrix (Weisberg et al. 2006). They do not contain organic matter in their matrix. The H (high-iron) group of OCs are characterized by their high siderophile element content, with a metal abundance of around 8 vol.%. Petrological type 6 designates chondrites that have suffered metamorphism under conditions sufficient to homogenize all mineral compositions, but melting did not occur and therefore there is no phase differentiation. KG 007 was obtained already grinded and in two different phases: one containing the full meteoritic composition (Sample B) and another one only containing the metallic inclusions separated by magnetic means (Sample C).

NWA 801 is a CC of subtype R and petrologic type 2 (Connolly Jr. et al. 2007). CCs are very primitive materials that have Mg/Si ratios near solar values and oxygen isotope compositions below the terrestrial fractionation line (Weisberg et al. 2006). The Renazzo subgroup (R) is distinguished by large and abundant porphyritic chondrules (50 vol.%). It has few refractory inclusions and an abundant metal percentage, between 5–8 vol.%, and a fine-grained matrix, which is commonly hydrated occupying up to 50 vol.%. As mentioned above, they are important because they contain up to 4% of organic matter aggregates in their matrix (Remusat et al. 2007; Alexander et al. 2017; Trigo-Rodriguez et al. 2019). Petrological type 2 designates chondrites characterized by abundant hydrated minerals and an abundant fine-grained matrix, with Ni-bearing sulfides. NWA 801 (Sample D) was obtained as a small chunk and was completely grinded before introducing it in the reactor, using a glass mortar until obtaining a very fine dust. Details on the petrology and composition of each chondrite type used in the samples can be found in Table 1.

For each sample, 0.5 g of meteoritic dust was mixed with 2.5 g of SiC, a very inert compound which assured a constant volume of the samples so the contact time between the reactants and the samples was optimized to maximize the reaction

Table 1. Average petrologic characteristics of the chondrite groups used in this work.

Type	Chondrule abund.$^{(*)}$ (vol.%)	Matrix abund. (vol.%)	CAI abund. (vol.%)	Metal abund. (vol.%)	Average chondrule diameter (mm)	Organic content (wt%)
CR	50–60	30–50	0.5	5–8	0.7	0.8–2.6
H	60–80	10–15	≪1	8	0.3	0

Notes. Adapted from Weisberg et al. (2006). $^{(*)}$Chondrule abundance includes lithic and mineral fragments.

Table 2. Sample description.

Sample	Meteorite	Type	Subtype	Weight (g)	SiC weight (g)	Total weight (g)	Gas flow
A	–	–	–	–	3.0027	3.0027	H_2/CO
B	KG007	OC	H6	0.5012	2.4996	3.0008	H_2/CO
C	KG007 (magnetic phase)	OC	H6	0.5158	2.4929	3.0087	H_2/CO
D	NWA 801	CC	CR2	0.5256	2.4814	3.0070	H_2/CO
E	NWA 801	CC	CR2	0.5060	2.4986	3.0046	Ar

Notes. Instrumental errors are ±0.0001 g.

rate, assure reproductibility and allow for a comparison between the samples. Details on the sample preparations can be found in Table 2. Sample A was used as the blank analysis in order to follow the progress of the reactions without meteoritical samples and to assure that there is no chemical activity coming from SiC. Sample E was used as a second blank analysis, with a meteoritical content from NWA 801 but without passing CO and H_2 as reactants and circulating Ar instead, in order to ensure that the detected products are not coming from the meteorite itself due to the presence of organic matter in the matrix of CCs. This procedure was not done for KG 007 because it is an OC and therefore it does not contain any organic matter in the matrix. Due to the relatively rare nature of the samples and the lack of enough material, we were unable to produce duplicates of each sample and of each experiment.

2.2. Fischer–Tropsch reactions

The reaction conditions were the same for all the samples. The total weight of the samples was introduced in a closed stainless-steel reactor with an internal diameter of 6 mm and a total volume of 5 mL and it was heated by a furnace, where a flux of CO and H_2 was circulated. The conditions were selected to resemble those present on the primitive surface of the Earth. The ratio of reactants was set to H_2:CO = 4, which is consistent with the estimated primitive ratios of the primitive atmosphere of Earth, that is H_2:CO = 0.03–10 (Kress & Tielens 2001). The fluxes of the reactants were set to a total of 40 mL min^{-1}, with H_2 = 32 mL min^{-1} and CO = 8 mL min^{-1}. For Sample E, Ar was circulated as an inert gas with a flux of 40 mL min^{-1}. Pressure was set to 1 atm to simulate the average pressure on Earth's surface. Since the relevant production of FTT reactions starts at 400 K (Sekine et al. 2006), here the temperature was increased manually from 200 to 600 °C in steps of 50 °C.

Products were analyzed online with an Agilent 3000A micro gas chromatography (GC) system. The GC is directly connected to the outlet of the reactor by stainless steel tubes. A schematic of the experimental setup is shown in Fig. 1. Three different columns were used in order to be able to analyze products with different polarities: an 8 m PLOTU for hydrocarbon analysis, a 10 m STABILWAX for oxygenated compound analysis, and a MS5A for nonpolar compound analysis. Each product was quantified with calibration standards and using the GC software *Soprane*. Standards and reaction gases were supplied by Nippon Gases and had a purity of 99.999%.

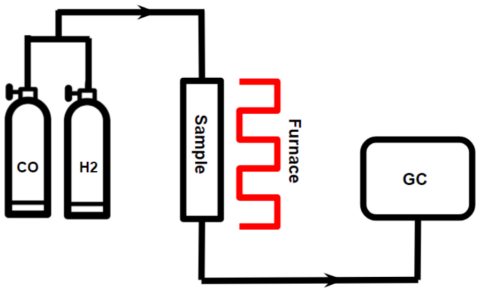

Fig. 1. Schematic of the experimental setup. The CO and H_2 were passed through the heated reactor containing the samples, and the resulting gas was injected into the GC.

Reactions were carried out during ca. 3 h, though the time varied depending on the stability of the production. Products were analyzed continuously, with injections to the GC every 5 min. After each experiment, the reactor was cleaned with a brush, using only water and then dried in an oven at 200 °C.

3. Results

In the present experiments, the production of hydrocarbons has been successfully achieved, in addition to other minor products such as primarily alcohols and other oxygenated compounds. The percentage of products obtained was computed as the percentage of CO that has been transformed in each different product, including the production of solid carbon, following Eq. (5):

$$\chi_P = \frac{n_P}{n_{CO,\,R}} \times 100 = \frac{n_P}{n^i_{CO} - n^f_{CO}} \times 100, \quad (5)$$

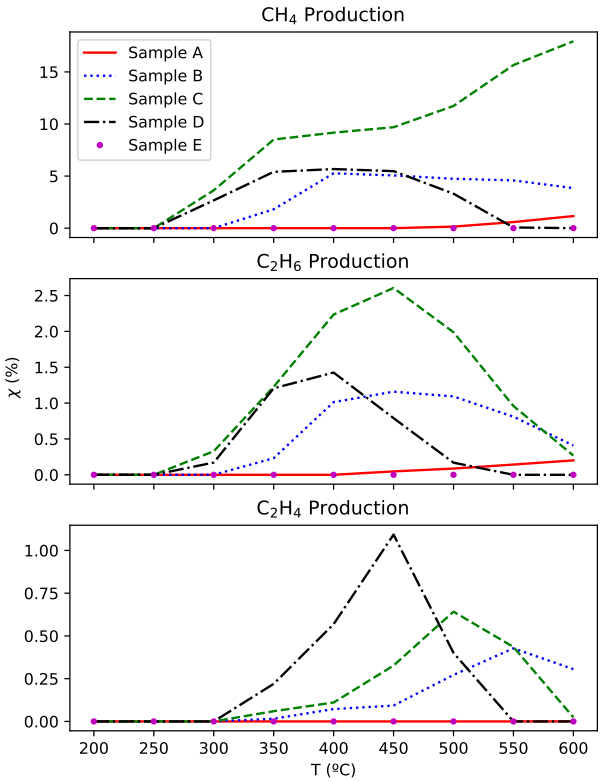

Fig. 2. Evolution of the production of hydrocarbons with temperature: CH_4 production (*top*), C_2H_6 production (*middle*) and C_2H_4 production (*bottom*).

where χ_P is the molar fraction of the formed product (in %), n_P is the obtained mols of the formed product, and $n_{CO,R}$ are the mols of CO that have been consumed, which were computed as the difference between the initial CO mols (n^i_{CO}) and the final CO mols detected (n^f_{CO}). The obtained chromatograms for all the experiments are shown in Appendix A.

3.1. Hydrocarbon production

Figure 2 shows the evolution of the production of the different hydrocarbons with temperature. In the different experiments, alkanes have been successfully synthesized, methane (CH_4) and ethane (C_2H_6) being the primary and the secondary products.

For Samples B–D, the formation of CH_4 starts at 300 °C. For Samples B and C, such a production still works at higher temperatures than 600 °C, while for Sample D it stops before reaching 550 °C.

The production of C_2H_6 also starts at 300 °C, but it decreases at 550–600 °C for Samples B and C. Whereas for Sample D, this happens at 400 °C.

The production of alkenes starts at a slightly higher temperature than that for alkanes (i.e., 350 °C). For Samples B and C, it starts to decrease when the temperature reaches 600 °C while for Sample D it stops before reaching 550 °C. The formation of C_2H_4 starts to be detected when some amount of C_2H_6 was produced and the maximum production of C_2H_4 occurs upon the decrease of C_2H_6 suggesting that both mechanisms are correlated, meaning that alkene formation starts when the amount of alkanes in the catalyst surface is large enough. The formation of alkynes is not detected, indicating that the energy barrier for the formation of the triple-C bond is not surmountable even in presence of the catalysts.

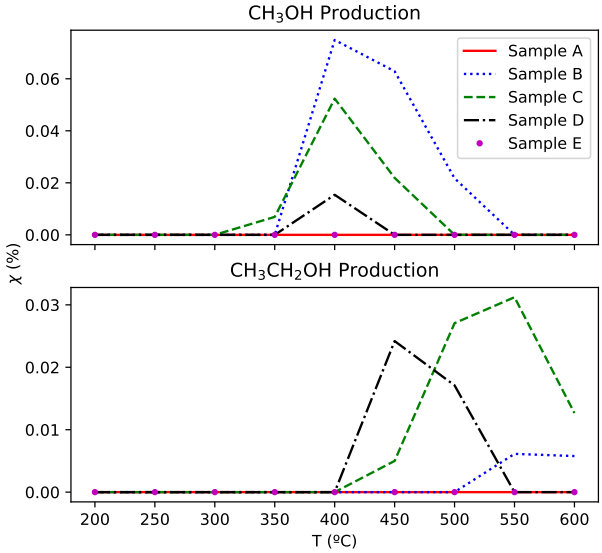

Fig. 3. Evolution of alcohol production with temperature. The CH_3OH production (*top*) and CH_3CH_2OH production (*bottom*).

For Sample A the production of alkanes and alkenes only start at higher temperatures than the other samples (at least 400 °C). Moreover, the percentage of the compounds formed are significantly smaller than in the presence of the meteoritical samples, being particularly evident for the most abundant products of the reaction (CH_4 and C_2H_6). These findings clearly provide evidence for the negligible activity of SiC and they suggest that the activity detected is caused by the reaction occurring in the meteoritical samples. Sample E shows no production of any of the aforementioned products, indicating that no desorption or outgassing of organics from the meteorite is detected under these conditions.

3.2. Alcohols production

Figure 3 shows the production of alcohols during the experiments. The profiles are rather different than those for hydrocarbon production. The formation of CH_3OH starts at 350 °C, peaks at 400 °C for all the samples, and it stops before reaching 550 °C, depending on the sample. The production of alcohols with longer carbon chains, mainly ethanol (CH_3CH_2OH), is restricted to higher temperatures, starting at 400 °C. The percentage of CH_3CH_2OH starts to increase when CH_3OH starts to decrease, indicating a sequential alcohol production (i.e., CH_3CH_2OH can only form when the concentration of CH_3OH is high enough). The maximum production is at 550 °C for all samples except Sample D, which occurs at lower temperatures (450 °C).

Some alcohols with even longer chains, such as propanol ($CH_3CH_2CH_2OH$) and butanol ($CH_3CH_2CH_2CH_2OH$), are detected, but only in a qualitative way. This indicates that the production of alcohols is not associated with the previous production of hydrocarbons so that both products are formed independently. No alcohols with an alkene chain have been detected, which sustains this hypothesis.

The production of alcohols does not take place in Sample A or Sample E. This suggests again that the products detected are being formed in the surface of the meteoritical material and that they are not coming from the activity of SiC or the meteorites themselves.

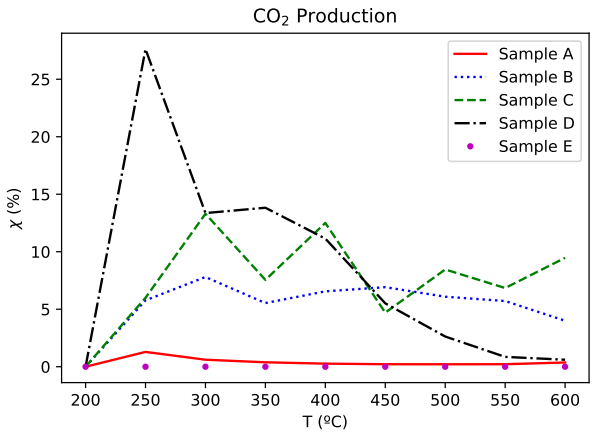

Fig. 4. Evolution of CO_2 production with temperature.

3.3. CO_2 production and carbon deposition

We note that CO_2 is continuously produced during the experiments, as shown in Fig. 4. Its production starts at 250 °C and it keeps relatively constant during all the experiment, the percentage of which depends on the sample. In view of that, CO_2 formation does not depend on the previous formation of hydrocarbons and/or alcohols. The production of CO_2 is not detected for Sample E, suggesting again there is no outgassing from the meteorite matrix.

The remaining percentage of the CO that has reacted but does not transform into products, and therefore does not appear in the percentage counting, is deposited on the surfaces of the meteoritical samples as solid carbon, poisoning the surfaces, and, with time, likely preventing FTT reactions from taking place in an efficient way (Llorca & Casanova 1998). The evolution of the surface poisoning is out of the scope of this paper.

3.4. Other compounds

Other compounds were detected during the experiments, but their evolution was not quantified. These compounds are mainly formaldehyde (H_2CO) and acetone ($(CH_3)_2CO$). They are formed at less than 400 °C, most possibly as byproducts or intermediates of the FTT reactions.

4. Analysis and discussion

4.1. Organic compound production on chondritic materials

In this work, it is proven that chondritic materials can support FTT reactions. First of all, it can be concluded that the organics detected do not come from the meteoritic samples. The non-detection of any products on the blank (Sample E) proves that the detected products are formed by the interaction of the reactants with the meteorite surfaces and that they do not come from the desorption or the outgassing of the meteorite matrix. We note other reasons that support that reactions are taking place in the reactor: (i) The progressive decrease in the amount of CO detected in the GC with respect to the initial CO introduced in the reactor suggests that the products are actually formed from the reactants and hence that they do not come from the meteorites themselves; (ii) the agreement of the distribution of products with the one expected from FTT reactions, the fact that no other species are detected, and the consecutive formation of products also indicate that the reactions are taking place on the surface of the meteorites; and (iii) if the products were coming from the samples, their production would not be detected over the extended time of the experiments. It should also be noted that while CCs do contain a very small amount of organic matter, and they could have been a possible source of contamination, OCs do not present any detectable percentage of organic material; accordingly, those detected here are being formed by processes occurring in the reactor.

It has also been checked that the reaction is not taking place because of the presence of SiC, by doing a blank analysis (Sample A). Those results show that the formation of hydrocarbons is negligible in comparison with the samples that present meteoritic material, especially for the most abundant products CH_4 and C_2H_6, and it only occurs at larger temperatures of at least 400 °C. Additionally, they do not show formation of alcohols, which is observed in the meteoritic samples. Overall, it is clear that the detected products are coming from reactions occurring inside the reactor and not from the samples themselves and that those reactions do not occur in the gas phase.

The total conversion of CO in products with respect to solid carbon is relatively low, less than 25%, but it is large enough to have quantitative results. In general, above 300 °C, the production of alkanes and alkenes is relatively important, with selectivities between 25 and 75% of the total product conversion (without accounting for solid carbon). Furthermore, CO_2 is also produced in large amounts, with a selectivity that goes down from 100 to 25% as the temperatures rises. Alcohols are also produced, but in minor quantities, with selectivities not larger than 0.6%. Nevertheless, their formation is very important because it demonstrates the incorporation of O in O_2-free environments, thereby forming polar groups that can result in molecules (i.e., $CH_3CH_2CH_2CH_2OH$ and larger alcohols) of great importance for prebiotic chemistry and biochemistry (Walde 2005).

This work allowed us to distinguish the differences between the two classes of chondrites (Samples B and D). The production of hydrocarbons starts at a slightly lower temperature for CCs than for OCs, though the percentage of products is roughly the same. The production of alcohols is similar as well, although it should be noted that Sample D produces a larger amount of CH_3CH_2OH. The similarities observed are attributed to the similar percentage of metallic inclusions in both chondrite types, while the differences are probably caused by their different metallic composition and the different alteration degrees suffered by the materials.

The activity of the metallic inclusions has been analyzed separately from the other phases (Sample C). The results indicate that the overall production is larger than for Samples B and D: it starts at lower temperatures and extends to larger temperatures. Some exceptions are noted: (i) The production of C_2H_4 is lower for Sample C than for Sample D (NWA 801), and (ii) the CH_3OH production is low in comparison to the other samples. We attribute both events to a possible different composition of the metallic phases, which can favor the formation of some products in detriment of others, that is the formation of C_2H_4 is not as favorable as C_2H_6 for the metals present in Sample C, while the formation of CH_3OH is reduced in favor of a larger and faster formation of CH_3CH_2OH. Although in this work is not possible to directly correlate and quantify the activity with the metal content due to the lack of prior characterization of the complete composition of the meteoritical samples, our findings suggest that the metallic phases are responsible for most of the surface activity of the samples, in detriment of the silicate phase. Moreover, previous experiments carried out by Ferrante et al. (2000), using silicate phase analogs alone, did not detect any FTT products,

supporting the hypothesis that the metallic phase (Fe in their case) was responsible for the chemical activity.

The results of the present work are in agreement with other works available in the literature. Under conditions resembling those of the solar nebula (pressure $\approx 10^{-4}$ atm and H_2:CO > 100:1), only hydrocarbons were produced, but with longer chains (C_1–C_4) (Llorca & Casanova 1998). When using Fe-doped silica instead, the experiments of Ferrante et al. (2000), which were carried out under similar conditions to this work (pressure ≈1 bar and H_2:CO = 2–100), produced a similar hydrocarbon distribution, finding CH_4, C_2H_6 and C_2H_4 as the most abundant products. However, they also conclude that the main activity occurred in the metallic phase. Other works also obtained more complex hydrocarbons under similar conditions (Gilmour et al. 2002), such as aromatic compounds, which have not been produced in this work. It should be noted that none of these works reported the production of alcohols or other oxygenated compounds.

The differences between the different works can be explained as follows. First, the experimental conditions are different. Here it is considered an Earth-like environment, that is to say larger pressures and H_2:CO = 4. As expected, larger pressures give faster reactions (reaction times of ∼3 h, this work and Ferrante et al. 2000 versus $>10^2$ h, Llorca & Casanova 1998). Moreover, our H_2:CO ratio probably favors the formation of alcohols in detriment of hydrocarbons (H_2:CO = 4, this work versus H_2:CO = 250, Llorca & Casanova 1998). Secondly, actual meteoritic samples are used while the cited works used synthetic metallic alloys. It is possible that alteration processes undergone by the meteoritic materials produced structural and electronic changes on their surfaces, giving rise to a different catalytic behavior. In addition, meteoritic materials do not only contain Fe in their composition, usually used as a metallic phase analog, but also other metals, such as Ni or Co, which are known to have an effect on the selectivity and product distribution of FTT reactions (Mahmoudi et al. 2017). This could favor the formation of oxygen-bearing compounds, which are not reported in other works. In order to totally understand the effect of the different alteration degrees of the samples in the chemical outcome and the actual relationship between the metal quantity and the catalytic activity, more similar experiments are needed using a more extensive sampling of chondrite types, which suffered different degrees of alteration and contain other and different amounts of metallic inclusions, such as CIs and CBs (which contain 0 vol.% and 60–80 vol.% abundance of metals, respectively).

4.2. The early Earth atmosphere and problems of the Fischer–Tropsch mechanism

One of the main conundrums to assess if these reactions could have taken place in an early-Earth environment relies on the real atmospheric composition at that time. The work by Miller and Urey (Miller 1953) assumed a strongly reducing atmosphere, composed of H_2, CH_4, NH_3 and H_2O, which is an ideal environment for FTT reactions. However, this vision has been questioned over the years. Based on geological arguments, the early atmosphere came from the degassing of Earth's interior, containing mainly CO_2, H_2O and N_2, which does not support the formation of CH_4 and NH_3 (Zahnle et al. 2010; Lammer et al. 2018; Gronoff et al. 2020).

Nevertheless, additional information on the processes that happened in the primeval Earth points to a more complex story. The first atmosphere probably contained gases trapped from the solar nebula during accretion, mainly H_2, CO, CH_4 and NH_3. In small planets, such as Earth, when the protostellar envelope vanishes the first atmosphere is likely to escape and outgassing of the planet forms the secondary atmosphere. The large amount of impacts during the formation of Earth could have helped the emergence of this atmosphere since the volatilization of parts of the silicates of the mantle could have allowed the presence of volatile elements, for example CO, in the atmosphere for a relatively long time (Lammer et al. 2018).

A consequence of these processes is that even though CO-containing atmospheres could not be stable, they probably existed as steady states for periods long enough so CO could react with H_2 triggering FTT processes, as well as other fundamental reactions such as the Haber-Bosch (HB) synthesis (i.e., ammonia formation from N_2 and H_2), thereby giving rise to a richer and more complex chemistry in the planet surface. These processes are envisioned to happen on vapor plumes produced after the impact of meteorites on Earth's surface (Trigo-Rodríguez & Martín-Torres 2013; Lammer et al. 2018), when reducing gases were locally released and the pressure and temperature were high enough.

5. Summary

In this work, FTT reactions have been investigated in the presence of different meteoritical samples and under conditions resembling those of the early Earth. These laboratory experiments demonstrate that the undifferentiated meteorites can act as a surface support to promote the synthesis of different organic compounds from H_2 and CO mixtures. The following conclusions have been reached:

- FTT reactions can occur under planetary conditions with the surface support of chondritic materials;
- FTT reactions under these particular conditions yield the synthesis of hydrocarbons (CH_4, C_2H_6 and C_2H_4) as well as alcohols (CH_3OH and CH_3CH_2OH) and other oxygenated compounds, such as H_2CO and $(CH_3)_2CO$ even in O_2-free reaction conditions. A large amount of CO_2 is also produced;
- The detection of products is associated with reactions happening on the surfaces of the meteorites and not due to the desorption of organic contents already present in the materials themselves. The activity is mainly associated with the metallic phases since they show larger productivity than other mineral phases (e.g., silicates).

We conclude that further work is needed to fully characterize the possible catalytic properties of different chondrite types, with a special focus on the influence of the different percentages of metal inclusions and different alteration degrees, and to determine if these materials can also promote other reaction-types crucial for prebiotic chemistry, such as the HB synthesis and further N_2 chemistry or sulfur- and phosphorous-based chemistry.

Acknowledgments. J.M.T.-R. acknowledges financial support from research project PGC2018-097374-B-I00, funded by FEDER/Ministerio de Ciencia e Innovación – Agencia Estatal de Investigación. J.L. is grateful to ICREA Academia program and funding from Generalitat de Catalunya (2017 SGR 128). A.R. is indebted to the "Ramón y Cajal" program, MINECO project CTQ2017-89132-P, DIUE project 2017SGR1323, and funding from the European Research Council (ERC) under the European Union's Horizon 2020 research and innovation programme (grant agreement no. 865657) for the project "Quantum Chemistry on Interstellar Grains" (QUANTUMGRAIN).

References

Alexander, C. M. O. D., Cody, G. D., De Gregorio, B. T., Nittler, L. R., & Stroud, R. M. 2017, Geochemistry, 77, 227

Bernstein, M. P., Dworkin, J. P., Sandford, S. A., Cooper, G. W., & Allamandola, L. J. 2002, Nature, 416, 401
Bianchi, E., Codella, C., Ceccarelli, C., et al. 2018, MNRAS, 483, 1850
Botta, O., & Bada, J. L. 2002, Surv. Geophys., 23, 411
Bottke, W., Vokrouhlicky, V., & Minton, D. e. a. 2012, Nature, 485, 78
Brearley, A. J., & Jones, R. H. 1998, Chondritic Meteorites, 36 (Washington, D.C., USA: In "Planetary Materials", Mineralogical Society of America), 3-1
Chuang, K.-J., Fedoseev, G., Ioppolo, S., van Dishoeck, E., & Linnartz, H. 2015, MNRAS, 455, 1702
Chuang, K.-J., Fedoseev, G., Qasim, D., et al. 2017, MNRAS, 467, 2552
Ciesla, F. J., & Sandford, S. A. 2012, Science, 336, 452
Connolly Jr., H. C., Smith, C., Benedix, G., et al. 2007, Meteorit. Planet. Sci., 42, 1647
Ehrenfreund, P., & Charnley, S. B. 2000, ARA&A, 38, 427
Elsila, J. E., Dworkin, J. P., Bernstein, M. P., Martin, M. P., & Sandford, S. A. 2007, ApJ, 660, 911
Enrique-Romero, J., Rimola, A., Ceccarelli, C., et al. 2019, ACS Earth Space Chem., 3, 2158
Fedoseev, G., Cupeen, H. M., Ioppolo, S., Lamberts, T., & Linnartz, H. 2015, MNRAS, 448, 1288
Fedoseev, G., Chuang, K. J., Ioppolo, S., et al. 2017, ApJ, 842, 52
Ferrante, R. F., Moore, M. H., Nuth, J. A., & Smith, T. 2000, Icarus, 145, 297
Gilmour, I., Hill, H. G. M., Pearson, V. K., Sephton, M. A., & Nuth, J. A. 2002, 33rd Annual Lunar Planet. Sci. Conf., March 11-15, 2002, Houston, Texas, 1613
Gronoff, G., Arras, P., Baraka, S., et al. 2020, J. Geophys. Res. Space Phys., 125, e27639
Herbst, E. 2017, Int. Rev. Phys. Chem., 36, 287
Ioppolo, S., Fedoseev, G., Chuang, K. J., et al. 2021, Nat. Astron., 5, 197
Krasnokutski, S. A., Jäger, C., & Henning, T. 2020, ApJ, 889, 67
Kress, M. K., & Tielens, A. G. G. M. 2001, MAPS, 36, 75
Lammer, H., Zerkle, A. L., Gebauer, S., et al. 2018, A&ARv, 26, 2
Lee, C.-W., Kim, J.-K., Moon, E.-S., Minh, Y. C., & Kang, H. 2009, ApJ, 697, 428
Linnartz, H., Ioppolo, S., & Fedoseev, G. 2015, Int. Rev. Phys. Chem., 34, 205
Llorca, J., & Casanova, I. 1998, MAPS, 33, 243
Llorca, J., & Casanova, I. 2000, MAPS, 35, 841
López-Sepulcre, A., Jaber, A. A., Mendoza, E., et al. 2015, MNRAS, 449, 2438
Mahmoudi, H., Mahmoudi, M., Doustdar, O., et al. 2017, Biofuels Eng., 2, 11
Martín-Doménech, R., öberg, K. I., & Rajappan, M. 2020, ApJ, 894, 98
McGuire, B. A. 2018, ApJSS, 239, 17
Miller, S. L. 1953, Science, 117, 528
Muñoz Caro, G. M., Meierhenrich, U. J., Schutte, W. A., et al. 2002, Nature, 416, 403
Nuevo, M., Auger, G., Blanot, D., & d'Hendecourt, L. 2008, Orig. Life Evol. Biosph., 38, 37
Oberg, K. I. 2016, Chem. Rev., 17, 9631
Remusat, L., Robert, F., & Derenne, S. 2007, Comptes Rendus Geosci., 339, 895
Rotelli, L., Trigo-Rodriguez, J. M., Moyano-Cambero, C. E., et al. 2016, Nat. Sci. Rep., 6, 38888
Ruzicka, A., Grossman, J. N., & Garvie, L. 2014, Meteor. Planet. Sci., 49, E1
Schulz, H. 1999, Appl. Catal., 186, 3
Sekine, Y., Sugita, S., Shido, T., et al. 2006, MAPS, 41, 715
Sephton, M. A. 2002, Nat. Prod. Rep., 19, 292
Shulze-Makuch, D., & Irwin, L. N. 2008, Life in the Universe (Heidelberg, Germany: Springer-Verlag)
Trigo-Rodriguez, J. M. 2015, Aqueous alteration in chondritic asteroids and comets from the study of carbonaceous chondrites, 15 (In "Planetary Mineralogy", European Mineralogical Union Notes in Mineralogy), 67
Trigo-Rodríguez, J. M., & Martín-Torres, F. J. 2013, Astrophys. Space Sci., 35, 85
Trigo-Rodriguez, J. M., Rimola, A., Tanbakouei, S., Cabedo Soto, V., & Lee, M. 2019, Space Sci. Rev., 215, 18
van Gelder, M. L., Tabone, B., Tychoniec, L., et al. 2020, A&A, 639, A87
Vasyunina, T., Vasyunin, A. I., Herbst, E., et al. 2014, ApJ, 780, 85
Walde, P. 2005, Prebiotic Chemistry (Berlin, Germany: Springer)
Weisberg, M. K., McCoy, T. J., & Krot, A. N. 2006, Meteorites and the Early Solar System II (eds. D. S. Lauretta & H. Y. McSween Jr.), University of Arizona Press, Tucson, 19
Zahnle, K., Schaefer, L., & Fegley, B. 2010, Cold Spring Harbor Perspectives in Biology
Zamirri, L., Ugliengo, P., Ceccarelli, C., & Rimola, A. 2019, ACS Earth Space Chem., 3, 1499
Zolensky, K., Krot, A. N., & Benedix, G. 2008, Rev. Mineral. Geochem., 88, 429

Appendix A: Experimental chromatograms

Table A.1. Guidance retention time for all the molecules detected by each GC column.

STABILWAX		PLOTU		MS5A	
Molecule	Ret. time (min)	Molecule	Ret. time (min)	Molecule	Ret. time (min)
H_2CO	0.55	C_2H_4	0.68	H_2	1.15
$(CH_3)_2CO$	0.65	C_2H_6	0.75	N_2	1.25
CH_3OH	0.70	CO	1.35	CH_4	1.75
CH_3CH_2OH	2.10			CO_2	2.00

Figures A.1 to A.15 show the chromatograms of each GC column for each sample analyzed and at each reference temperature. Table A.1 shows a guidance to the retention times used to assign the detected peaks. We note that the different GC columns have different baselines levels, but each analysis has been carried out with respect to the correspondent level, and therefore there should not be any baseline effects in the computed product percentage.

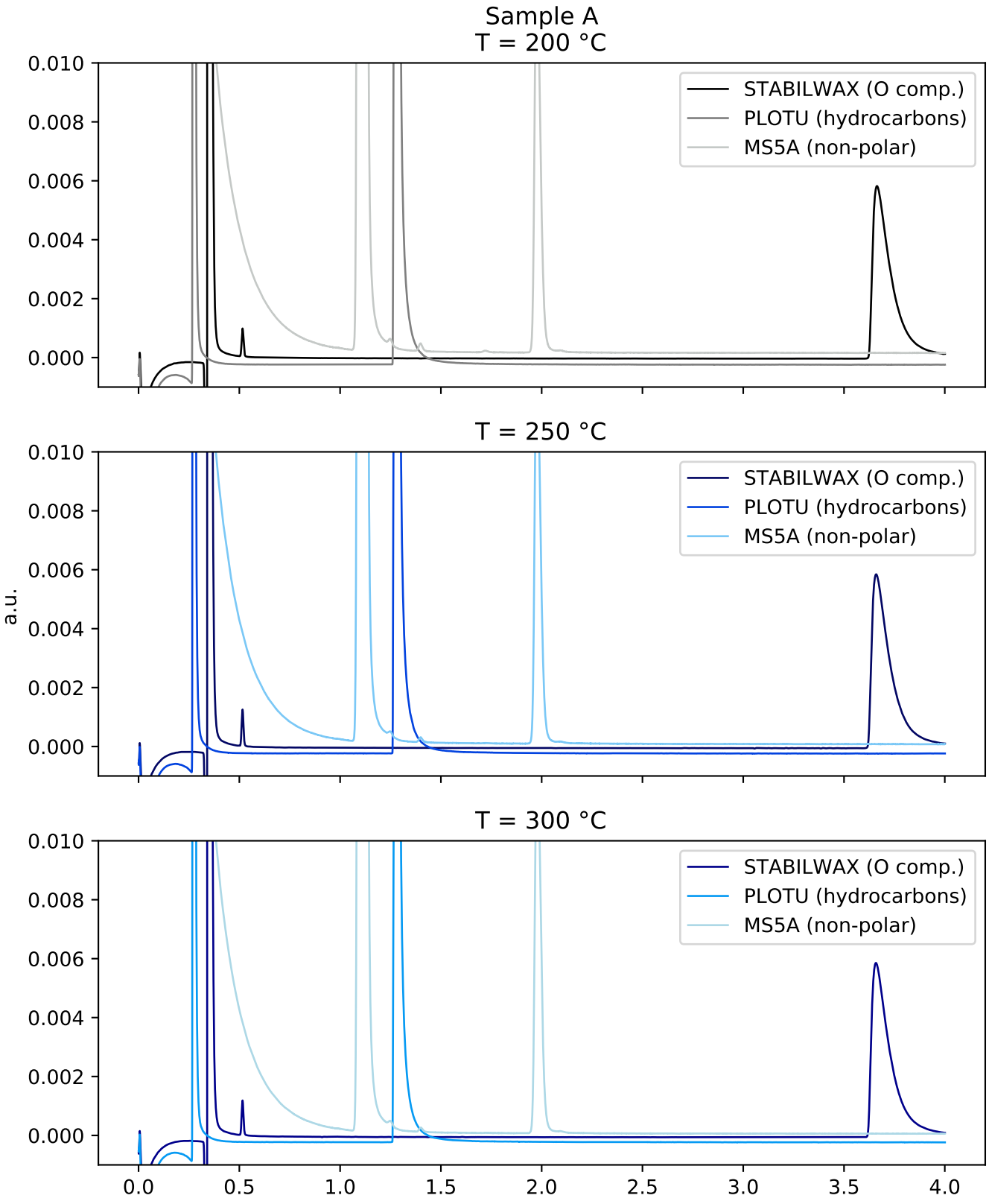

Fig. A.1. Normalized chromatograms at 200, 250, and 300 ,°C for Sample A.

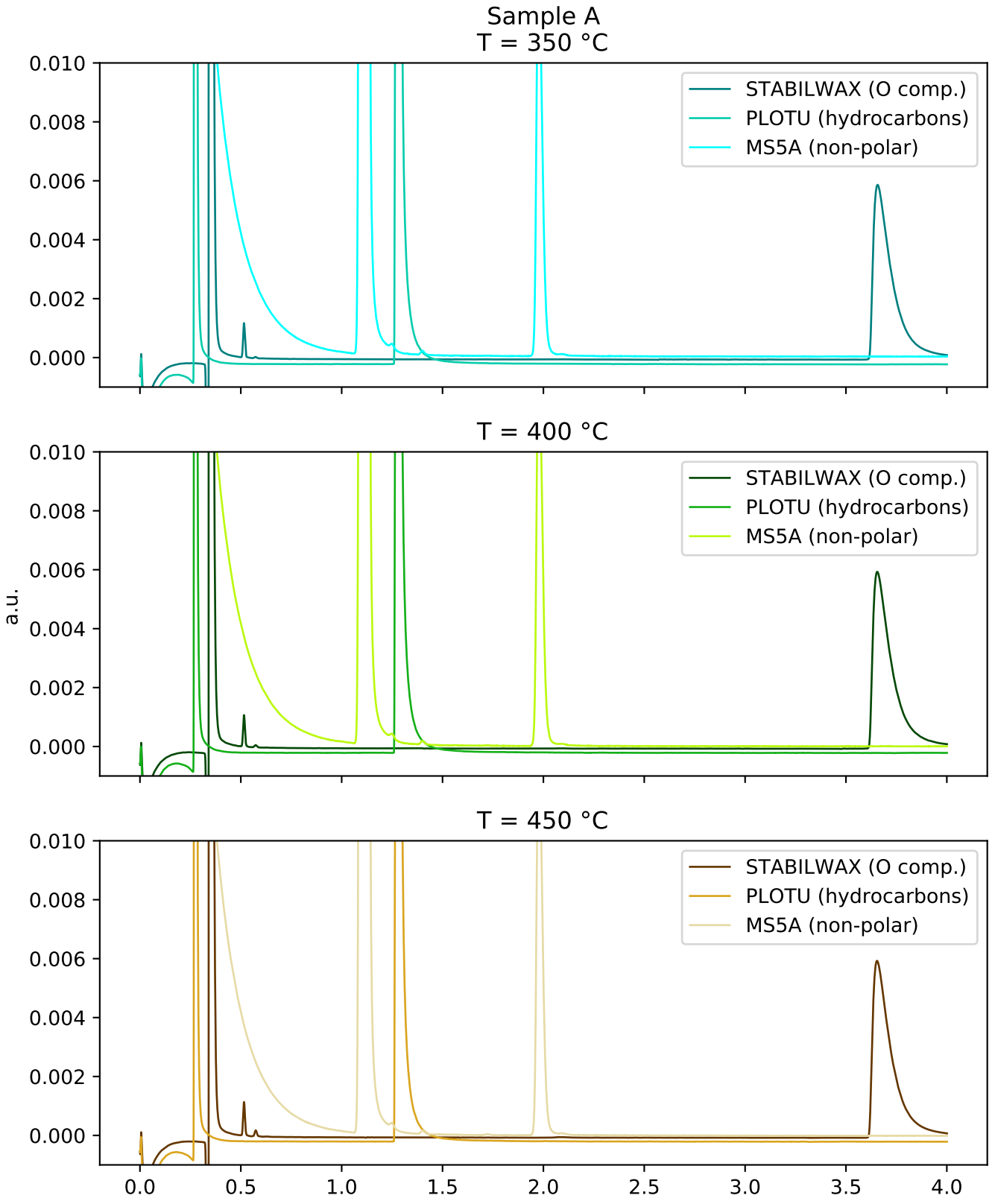

Fig. A.2. Normalized chromatograms at 350, 400, and 450 °C for Sample A.

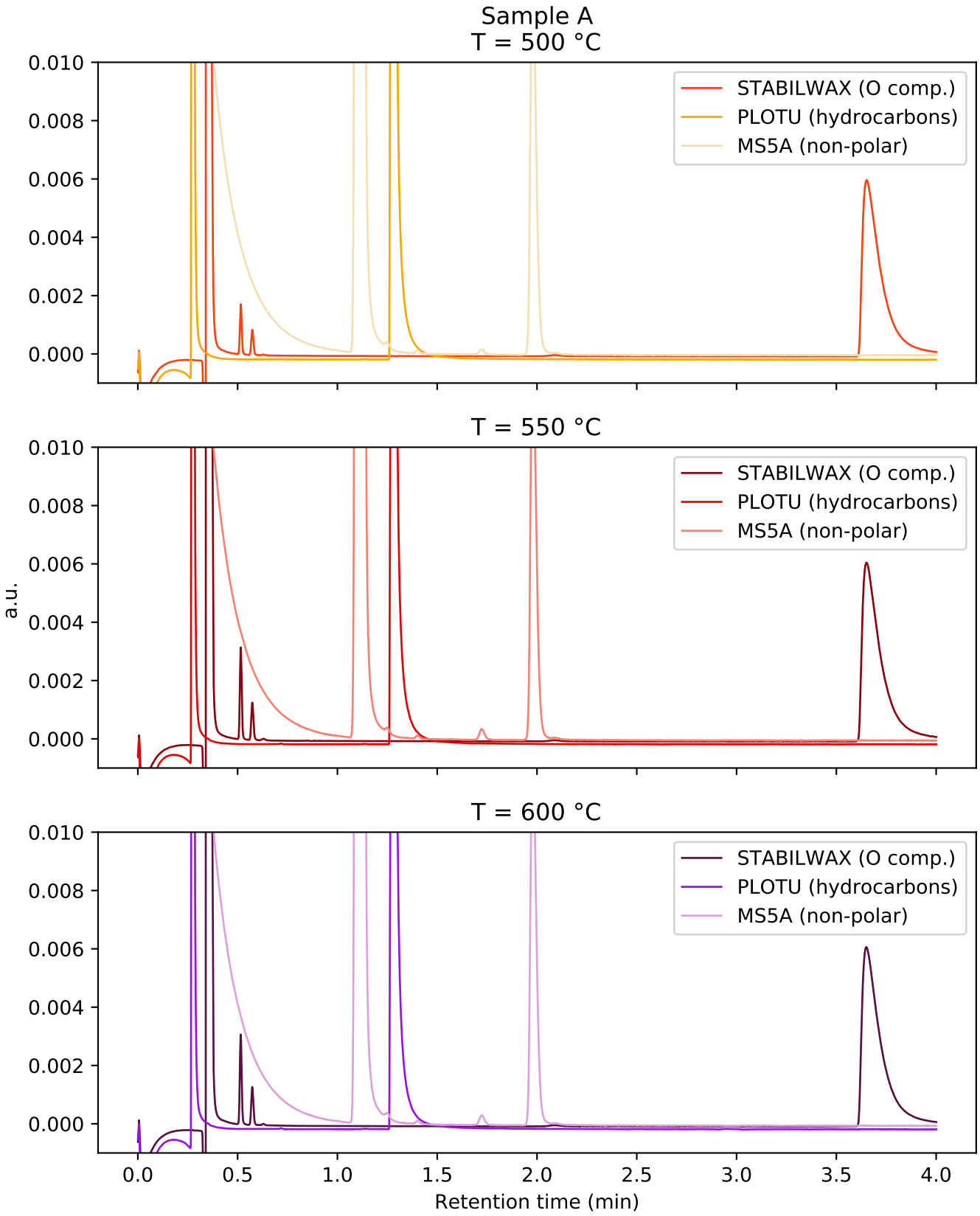

Fig. A.3. Normalized chromatograms at 500, 550, and 600 °C for Sample A.

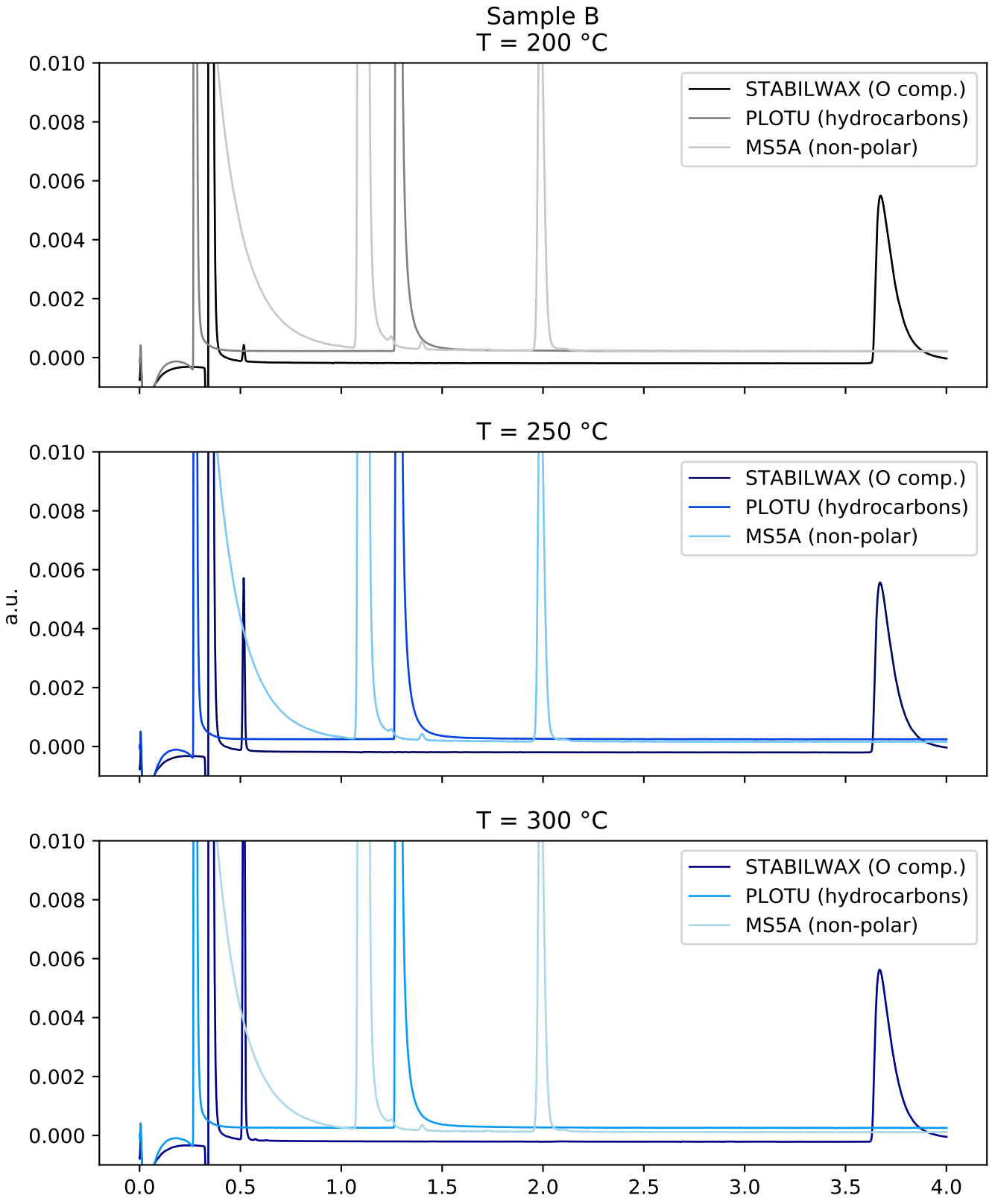

Fig. A.4. Normalized chromatograms at 200, 250, and 300 °C for Sample B.

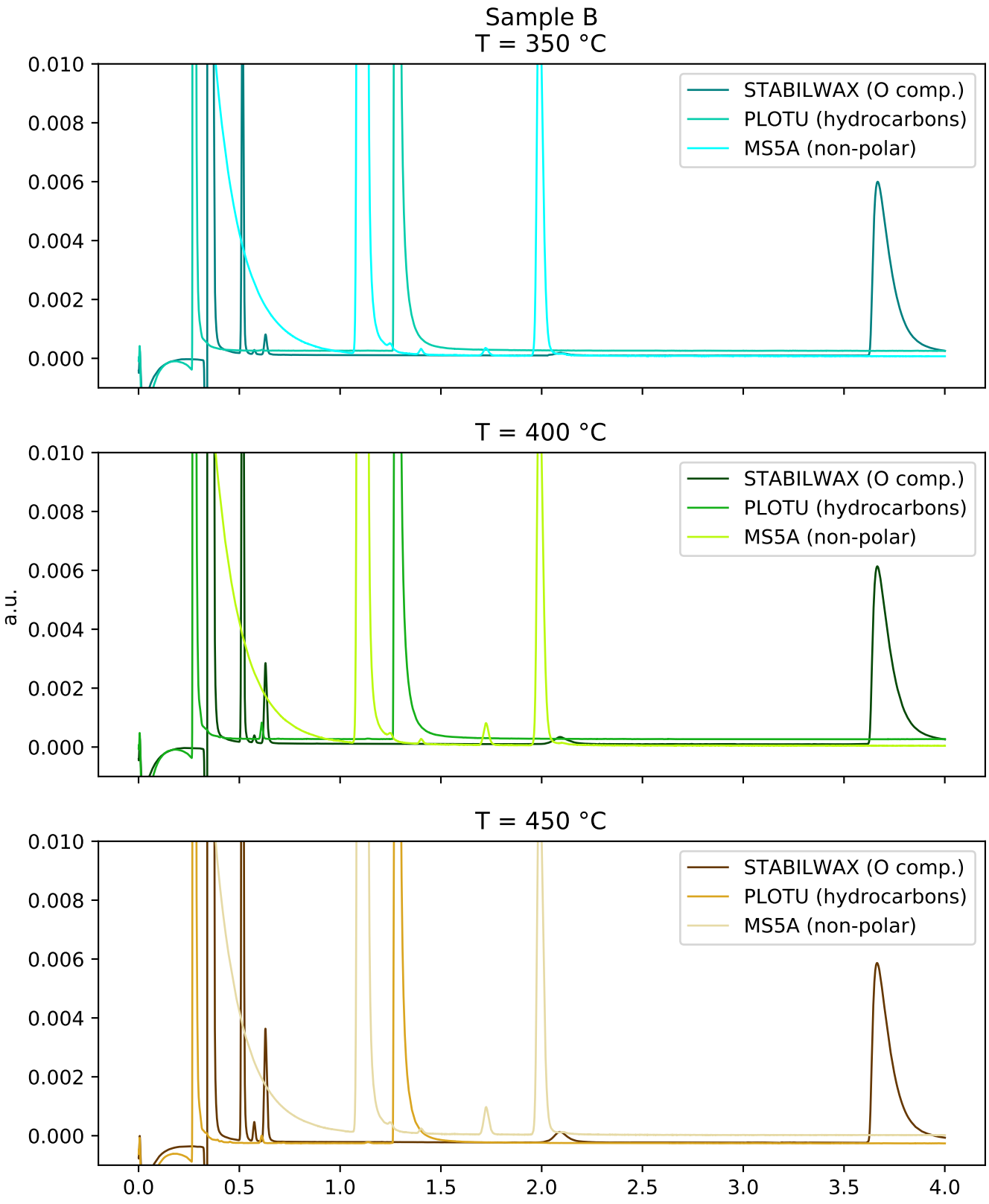

Fig. A.5. Normalized chromatograms at 350, 400, and 450 °C for Sample B.

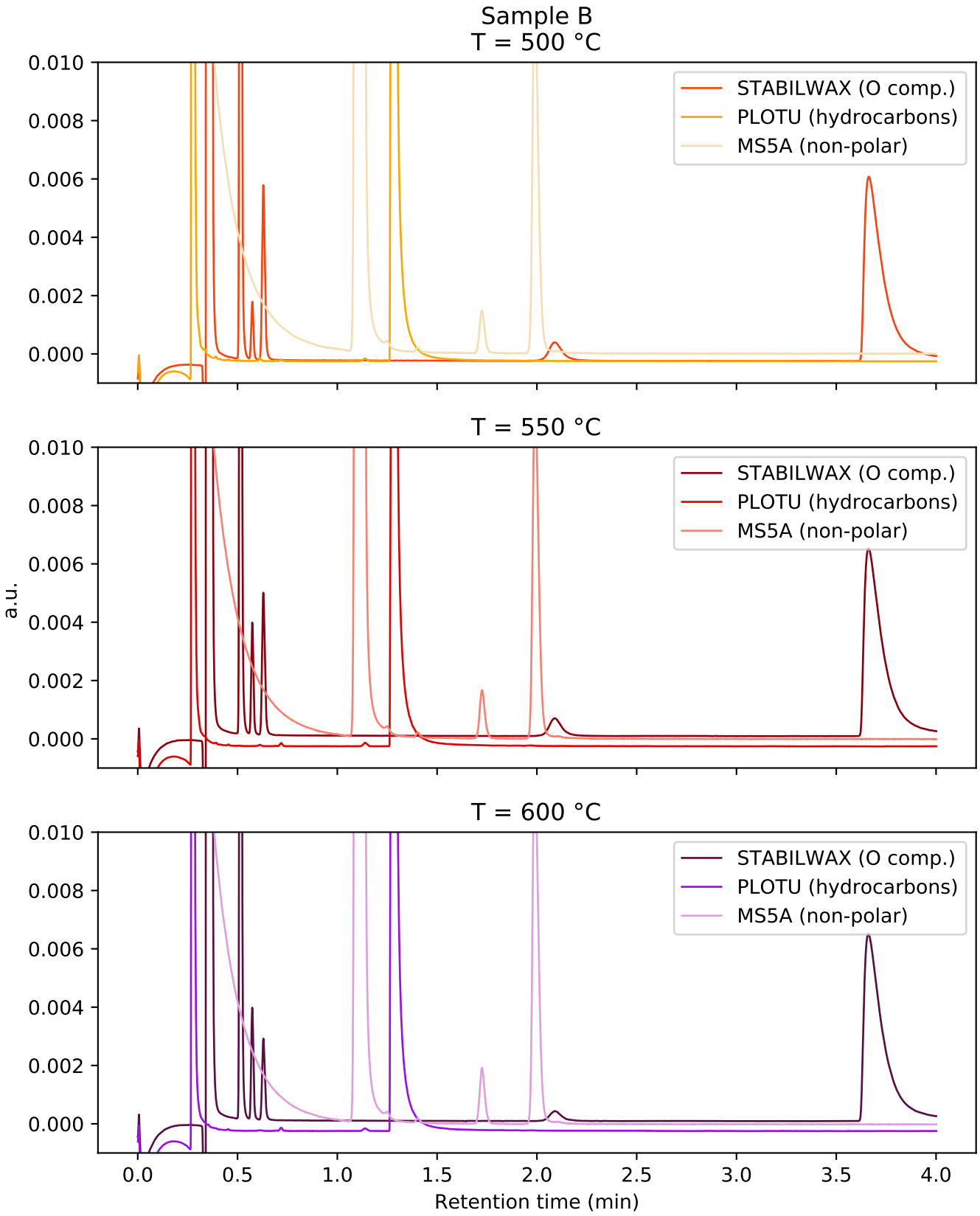

Fig. A.6. Normalized chromatograms at 500, 550, and 600 °C for Sample B.

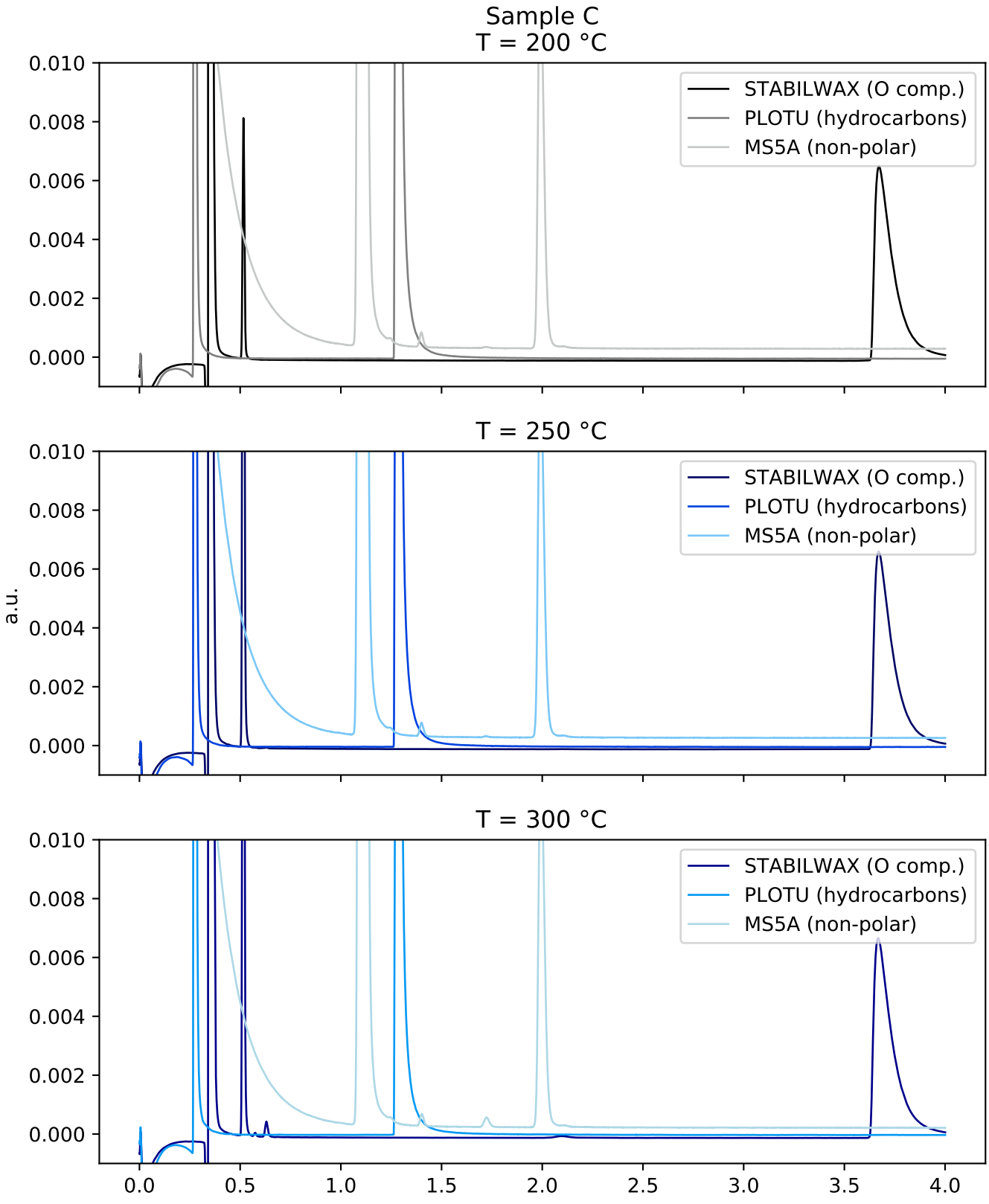

Fig. A.7. Normalized chromatograms at 200, 250, and 300 °C for Sample C.

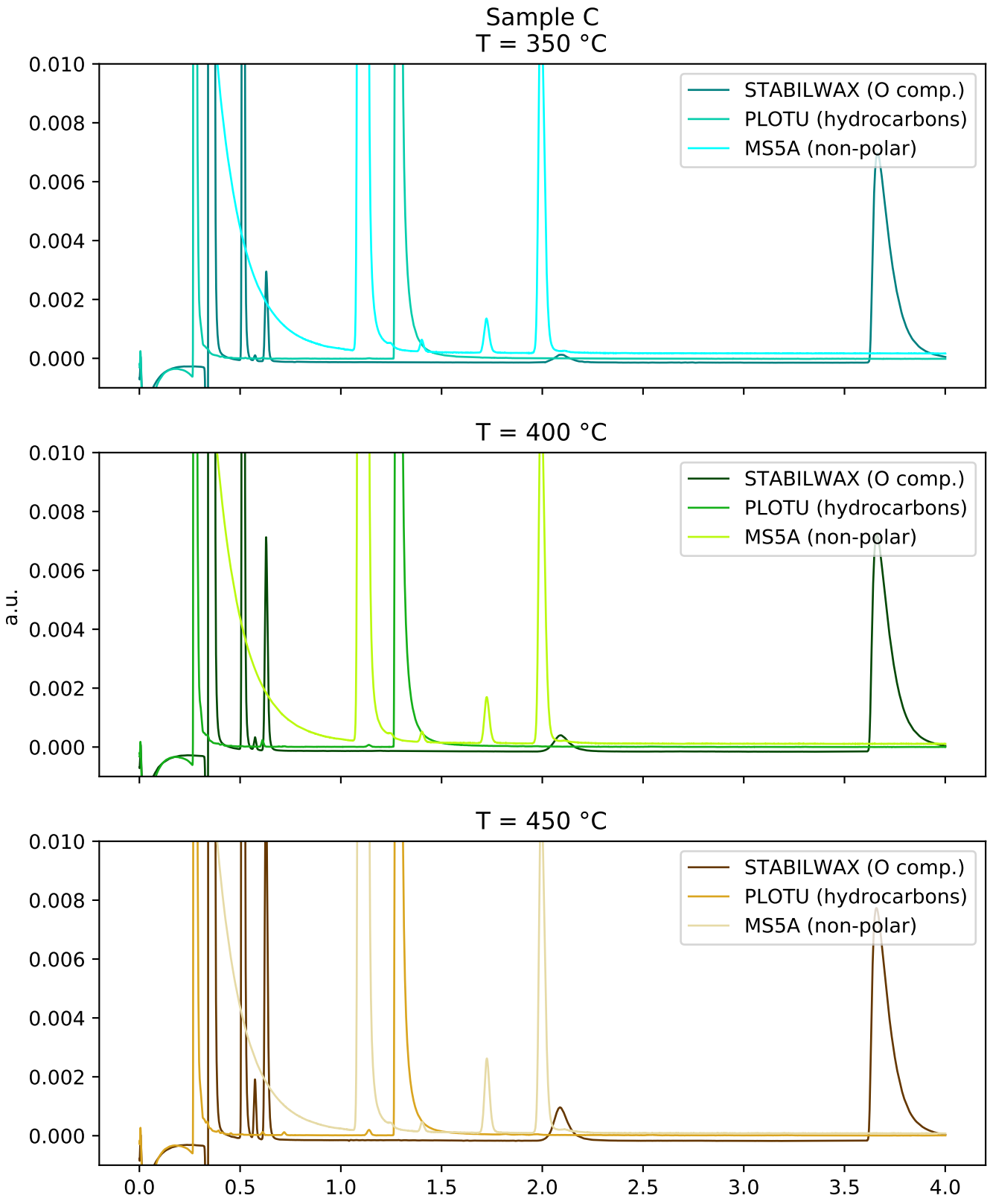

Fig. A.8. Normalized chromatograms at 350, 400, and 450 °C for Sample C.

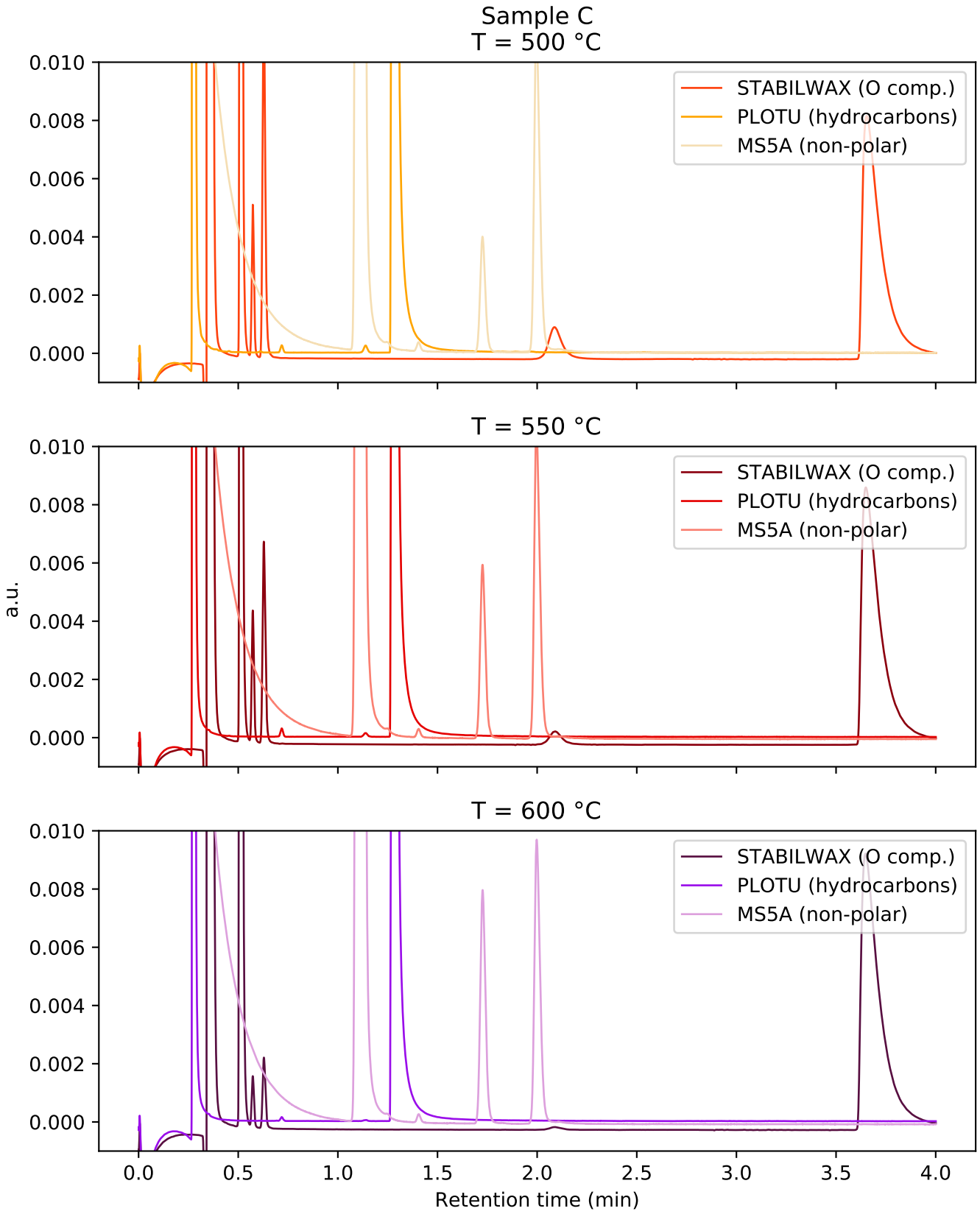

Fig. A.9. Normalized chromatograms at 500, 550, and 600 °C for Sample C.

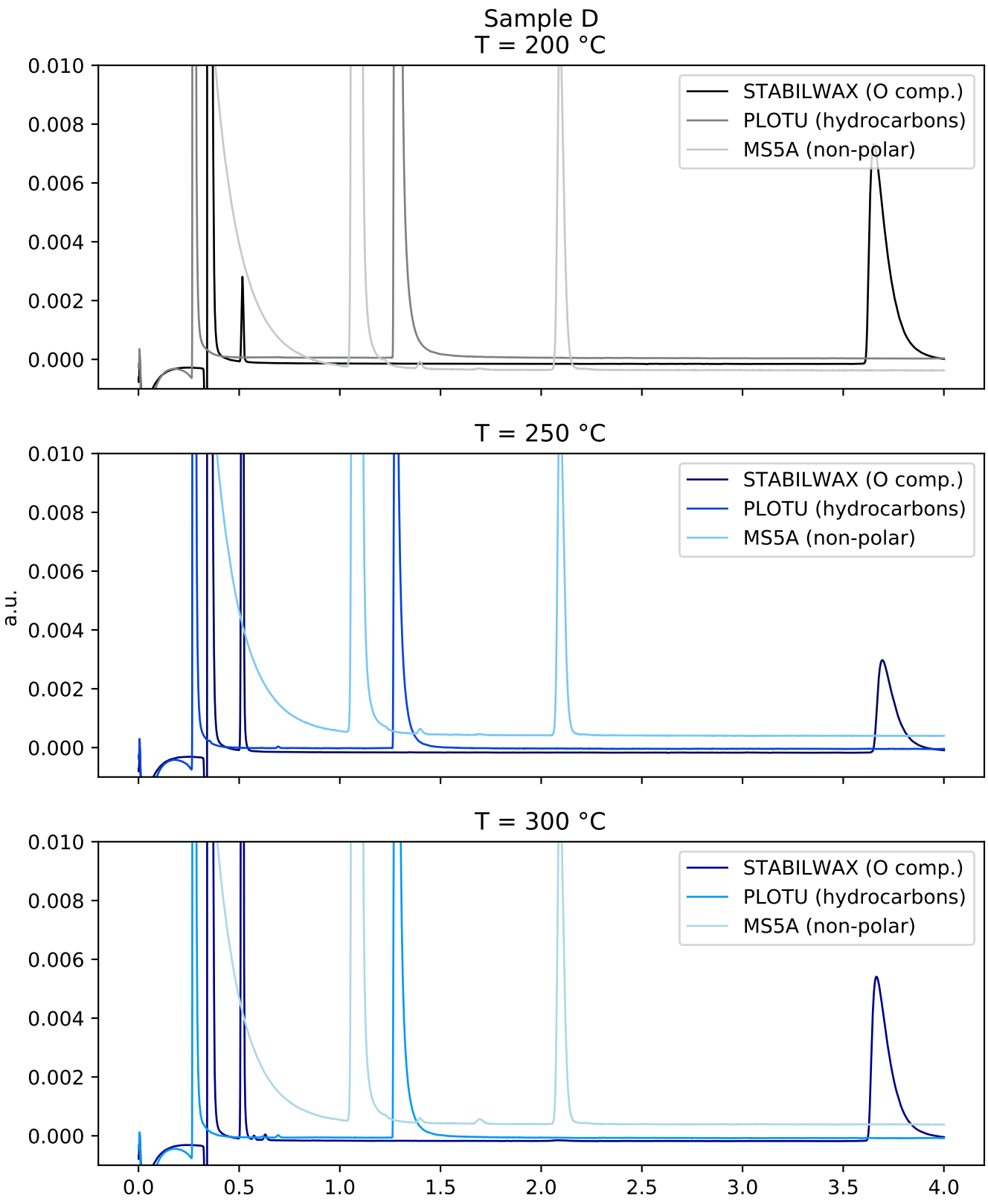

Fig. A.10. Normalized chromatograms at 200, 250, and 300 °C for Sample D.

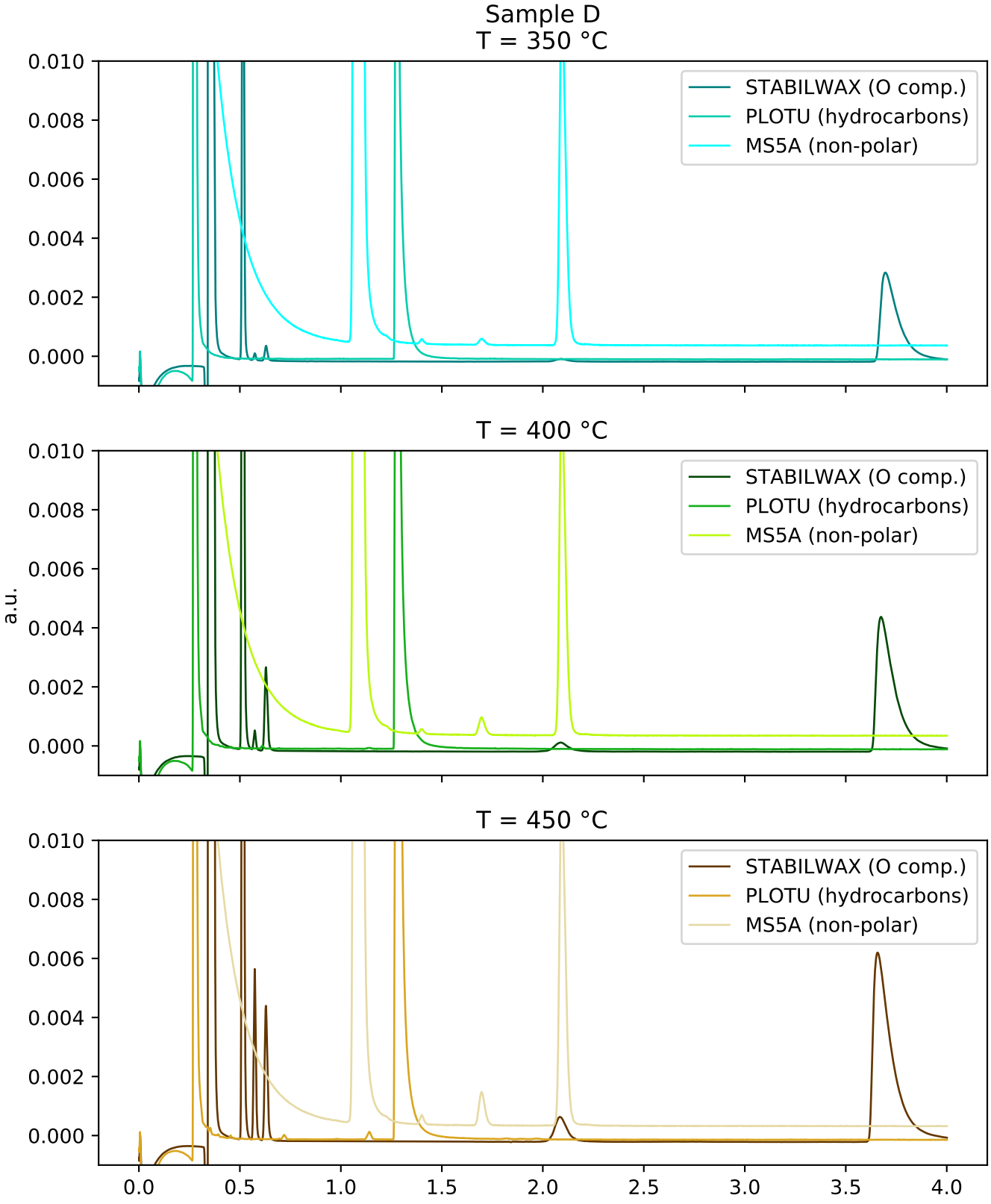

Fig. A.11. Normalized chromatograms at 350, 400, and 450 °C for Sample D.

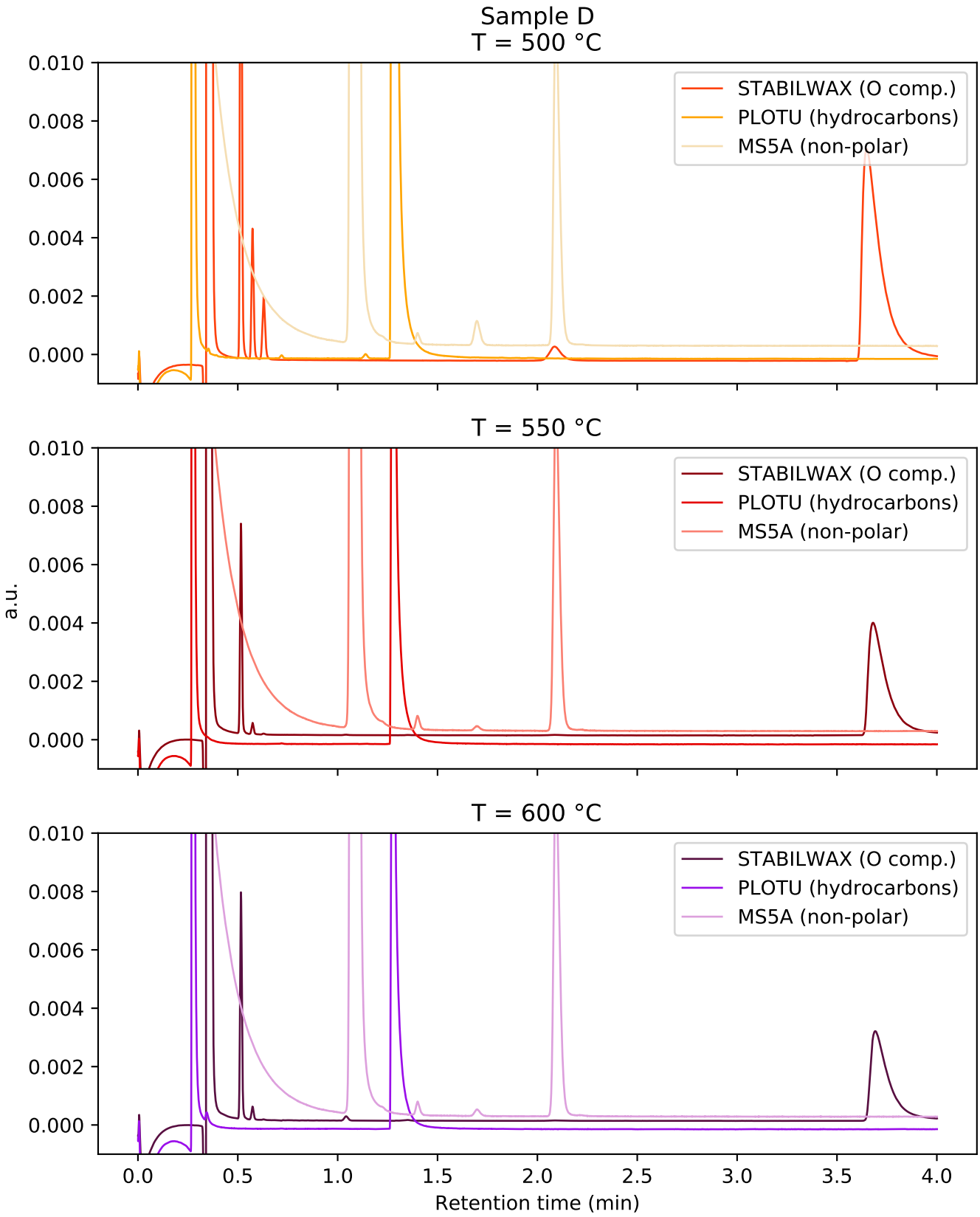

Fig. A.12. Normalized chromatograms at 500, 550, and 600 °C for Sample D.

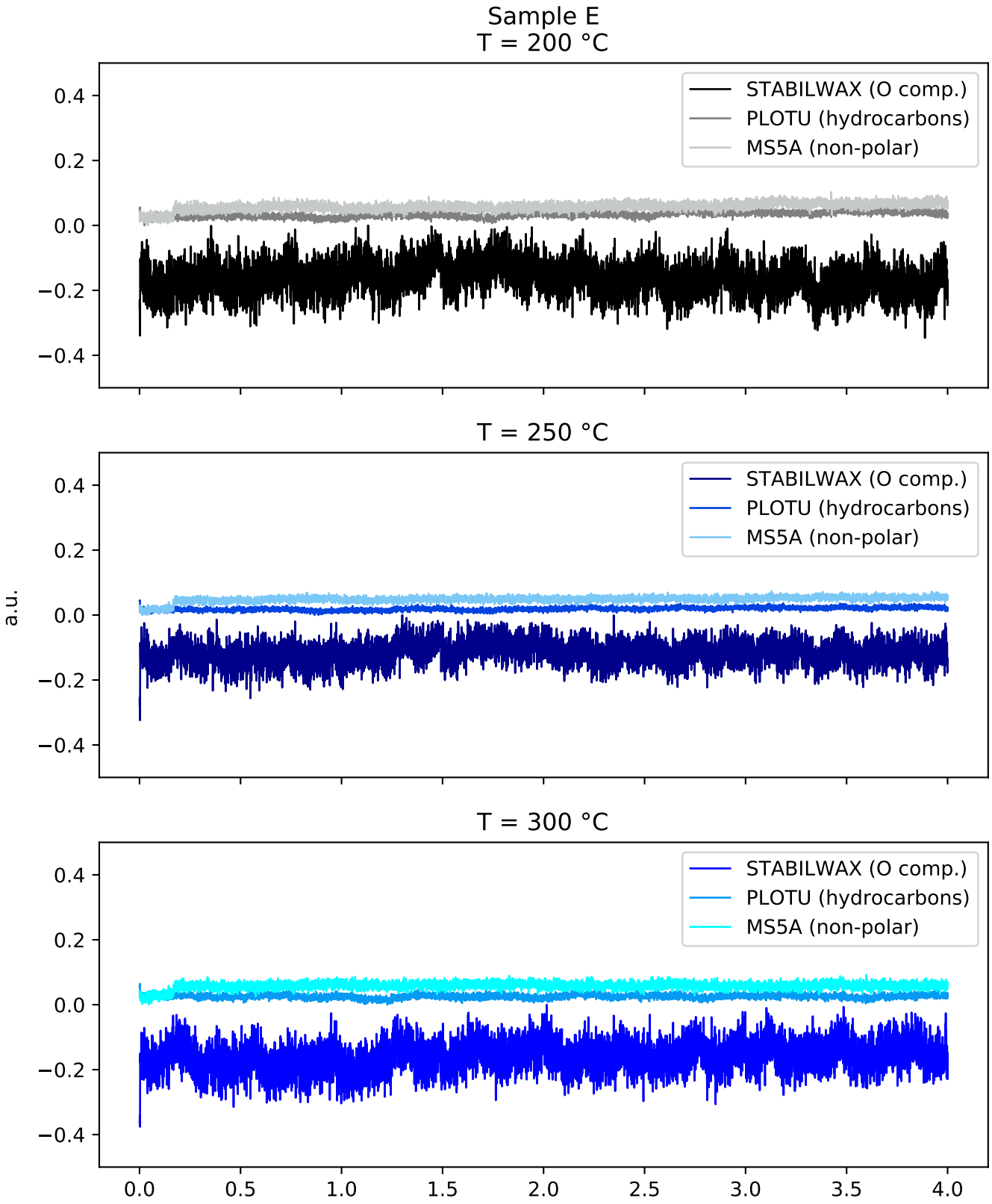

Fig. A.13. Normalized chromatograms at 200, 250, and 300 °C for Sample E. The plot shows only noise due to the lack of any reactant gas or product detected.

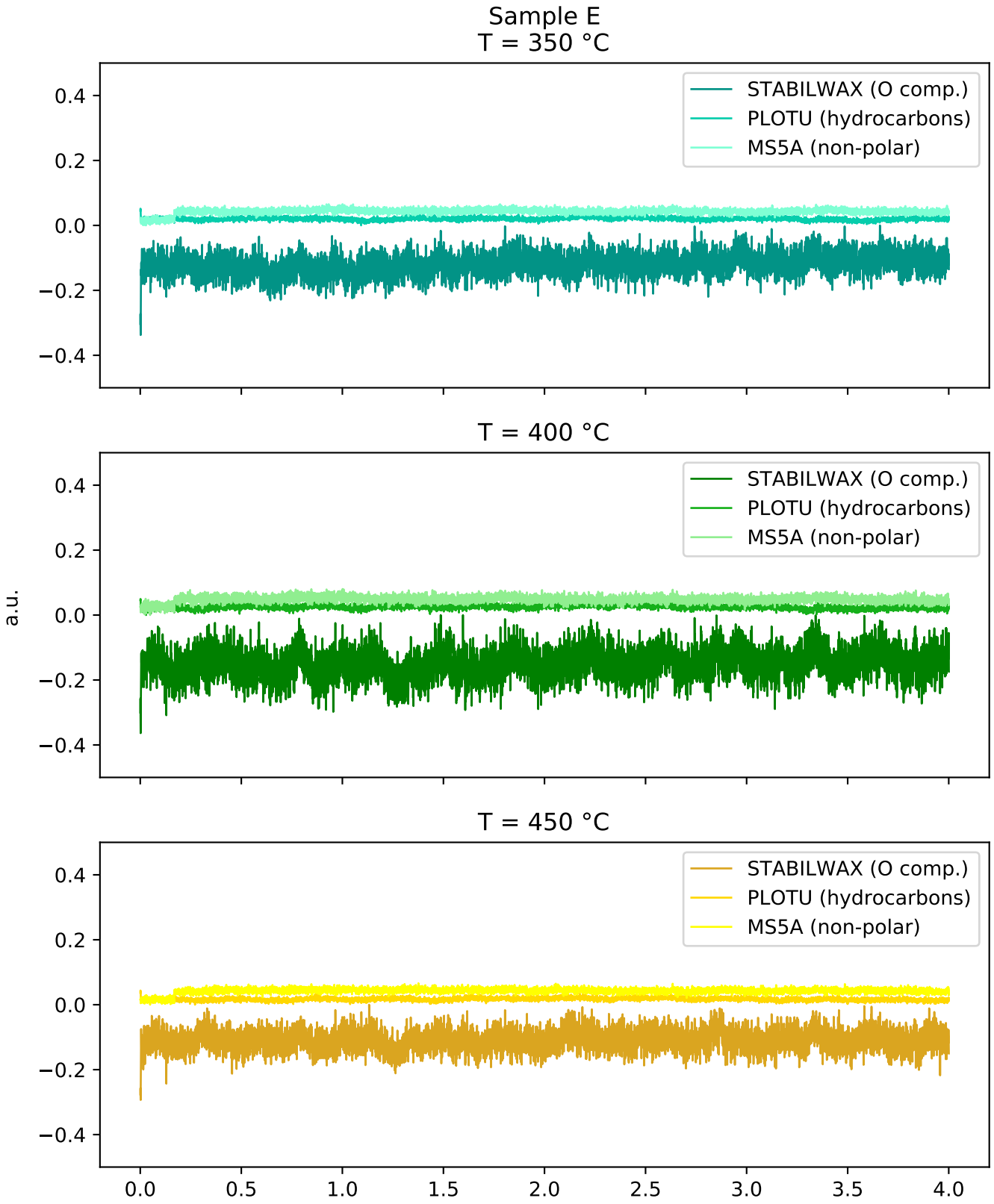

Fig. A.14. Normalized chromatograms at 350, 400, and 450 °C for Sample E. The plot shows only noise due to the lack of any reactant gas or product detected.

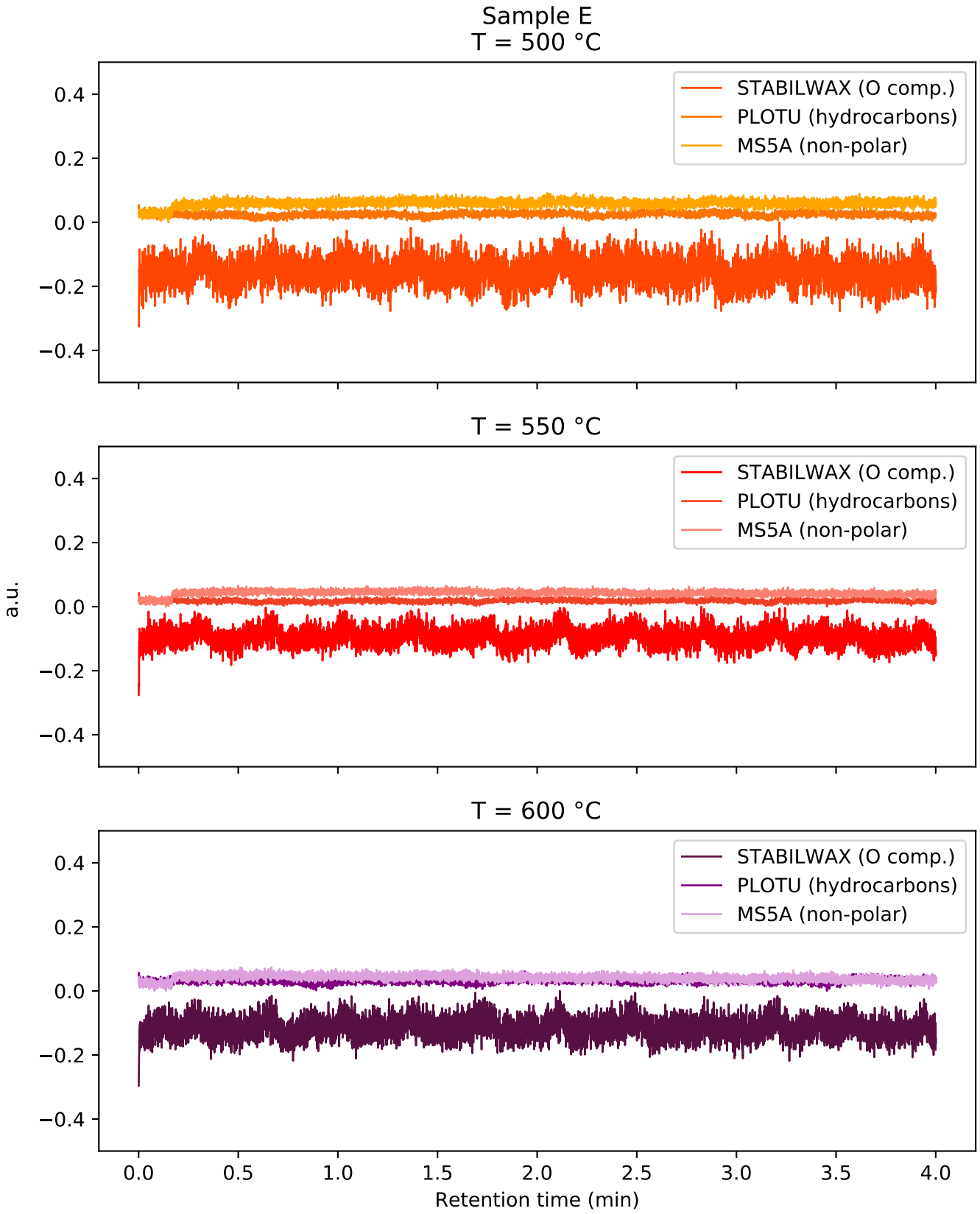

Fig. A.15. Normalized chromatograms at 500, 550, and 600 °C for Sample E. The plot shows only noise due to the lack of any reactant gas or product detected.